IMEKO 24th TC3, 14th TC5, 6th TC16 and 5th TC22 International Conference
11 – 13 October 2022, Cavtat-Dubrovnik, Croatia

RESEARCH ON PIEZO-ELECTRIC MATERIALS TO BE USED IN PRESSURE MEASUREMENTS

S. Molto[1], T. Rubin[2]

Centro Español de Metrología, Tres Cantos, Spain, [1] smolto@cem.es
Physikalisch-Technische Bundesanstalt (PTB), Berlin, Germany, [2] tom.rubin@ptb.de

Abstract:
Quantum-based methods have the potential to become primary standards for the SI unit of pressure, the pascal. Some of these standards are based on the determination of the refractive index of a gas under different pressure conditions by Fabry-Perot (FP)-based refractrometry methods. These methods depend on the control of other quantities, mainly the temperature and the mechanical stability. Ideally, the use of an improved cavity with piezo-electric and elasto-optic characteristics will allow for a novel and improved control of the effects of these parameters.

Keywords: Pascal; refractometry; pressure; piezo-electric; elasto-optic

1. INTRODUCTION

This research complements the QuantumPascal project targeting the quantum-based realization of pressure [1], [2]. It is focused on the design of Fabry-Perot cavities (FPCs) based on piezo-electric and elasto-optic materials in order to offer a better control of key parameters that are essential for the pressure assessment using FP refractrometry like mechanical deformations, temperature changes, etc. [3], [4].

Three possible set-ups are proposed:

1. FP-based refractrometry measuring the refractivity of a gas using a piezo-electric or elasto-optic cavity to correct parameters such as the deformation.
2. FP-based refractrometry measuring the refractivity of a piezo-electric or elasto-optic crystal.
3. Voltage measurements of a piezo-electric material using refractrometry to correct the corresponding parameters.

2. INITIAL REASEARCH

A total of 17 elasto-optic and piezo-electric materials were proposed in this initial research. Two parameters were calculated for each material using simulations: The voltage generated by an ideal parallel face capacitor and the changes in optical path length induced by pressure changes. These parameters are calculated using equation (1) and (2) respectively, where Q_i is the charge inside the capacitor, C is the capacitance, d_{ij} is the piezo-electric tensor, T_j is the stress applied, L_i is the length in the direction i, n_i is the refractive index in the i direction, p_{ij} is the elasto-optic strain tensor, S_j is the strain, C_{ij} is the stiffness tensor, L_i^{cal} is the calibrated length of the sample and $L_{Op\beta}$ is the optical path length. The knowledge needed to operate with the piezo-electric and elasto-optic tensors was acquired from the literature [5], [6], [7], [8], [9].

$$V_\beta = \frac{Q_\beta}{C} = \sum_{\alpha=1}^{6} \frac{\mathrm{d}_{\beta\alpha} T_\alpha}{\epsilon_0 \epsilon_{\mathrm{r}\beta}} L_\alpha \tag{1}$$

$$L_{OP\beta} = 2n_\beta L_\beta = 2\left(\frac{1}{n_\beta^2} + \sum_{\mathrm{j}=1}^{6} \mathrm{p}_{\alpha\mathrm{j}} S_\mathrm{j}\right)^{-\frac{1}{2}} \cdot \cdot \left(\left(\sum_{\mathrm{k}=1}^{6} \mathrm{C}_{\alpha\mathrm{k}}^{-1} T_\mathrm{k}\right) L_\beta^{cal} + L_\beta^{cal}\right) \tag{2}$$

The sensitivities for the voltage caused by applied pressure (θ_V) and the relative change in optical path length with respect to the applied pressure (θ_{OP}) are calculated using equations (3) and (4) where T is the applied pressure, V is the generated voltage due to piezo-electric effect, L_{OP} is the optical path length when pressure is applied and $L_{OP(0)}$ is the optical path length in the vacuum. The results of these calculations are shown in Figure 1 for the voltage sensitivity and in Figure 2 for the sensitivity with respect to changes in optical path length. As the piezo-electric and elasto-optic effects are no isometric effects, only the largest voltage obtained for each material is shown in Figure 1. In Figure 2 the value of θ_{OP} for the three main directions with respect to the dielectric matrix are shown (xx, yy, zz).

$$\theta_V = \frac{\partial V}{\partial T} \tag{3}$$

$$\theta_{OP} = \frac{\partial\left(\frac{L_{OP} - L_{OP(0)}}{L_{OP(0)}}\right)}{\partial T}. \quad (4)$$

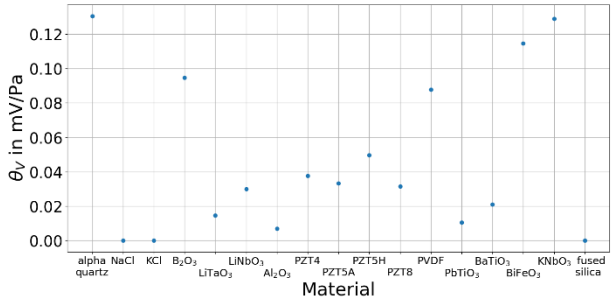

Figure 1: Sensitivity (voltage generated) with respect to the applied pressure for the 17 preselected materials.

The material with highest sensitivity is the Quartz (SiO_3), which is the most common piezo-electric crystal. Also, the PVDF (Polyvinylidene fluoride) has a high piezo-electric effect, and is a polycrystalline material. Although $BiFeO_3$, $KNbO_3$, B_2O_3 have high sensitivities but there are only a few information about them in the literature.

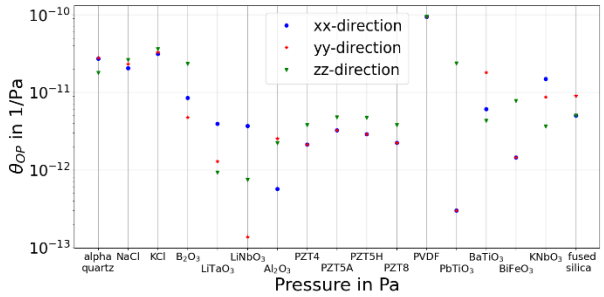

Figure 2: Sensitivity of relative change in optical path length due to pressure for the 17 preselected materials.

PVDF will lead to the largest relative change in optical path length. But this is caused by the deformation of the material and not by the elasto-optic effect. Sapphire (Al_2O_3) has one of the smallest sensitivities. However, it has the lowest pressure deformation, so most of the relative change in optical path length is due to the elasto-optic effect.

Analysing the results of the figures, three materials were selected to be further investigated within the scope of our project: Quartz (SiO_2), Sapphire (Al_2O_3), and PVDF (Polyvinylidene fluoride).

PVDF does not have well known elasto-optic properties, though its piezo-electric behaviour can be used only in two of the three proposed approaches.

3. THREE APPROACHES

3.1. First Approach

The optical design used for this approach is presented in Figure 3 where the measurement is made using the reflexions from the spacer. Here it is possible to observe an interference pattern even without HR coatings, since the reflexions from both surfaces (front and backside) are similar in power.

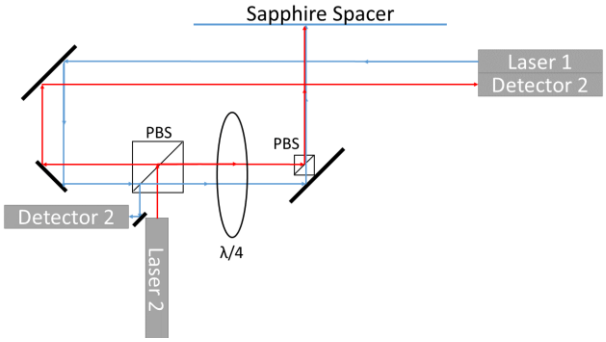

Figure 3: Sketch of the optical set-up utilizing a pure sapphire block to assess temperature changes.

The simulated cavity has the design shown in Figure 4A, which is similar to the design of the sapphire cavity used at the PTB (Figure 4B) but with less details. Sapphire is a birefringent material, so the refractive index depends on the direction of the beam compared to orientation of the spacer. Sapphire only has 1 main direction with a different refractive index (C-Axis), the spacer was designed to have that direction in the vertical axis, like in the corresponding experimental setup.

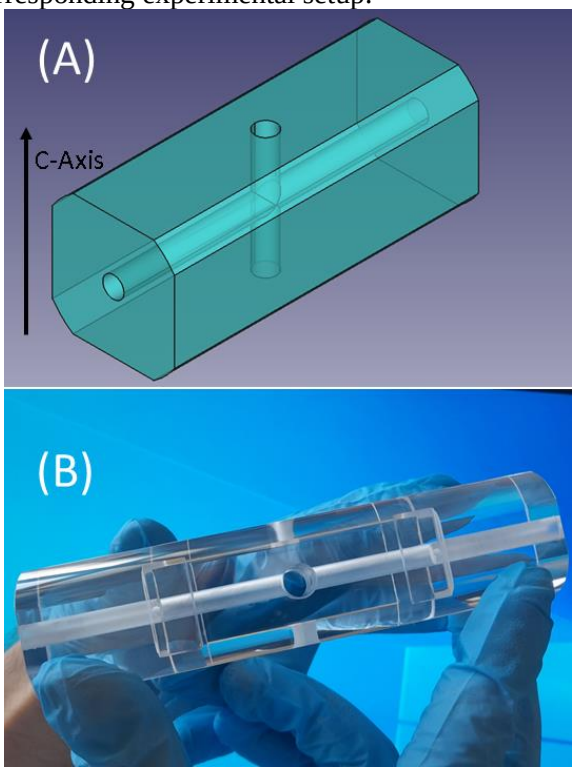

Figure 4: Image of (A) the simulated cavity and (B) the sapphire spacer at the PTB.

The results of the change in the beat frequency between an iodine-stabilised HeNe-laser and a horizontal polarized beam from a diode laser locked to the optical path length inside the spacer as well as the change between two locked diode lasers (one polarized horizontally and the other vertically

matching the axis of the spacer) with the temperature are shown in Figure 5. A linear behaviour is shown for both axis of the birefringent material. While the change in the refractive index is different for both directions. The change of the beat frequency between the two diode lasers is smaller than the change of the beat frequency between the iodine-stabilised HeNe-laser and the diode laser.

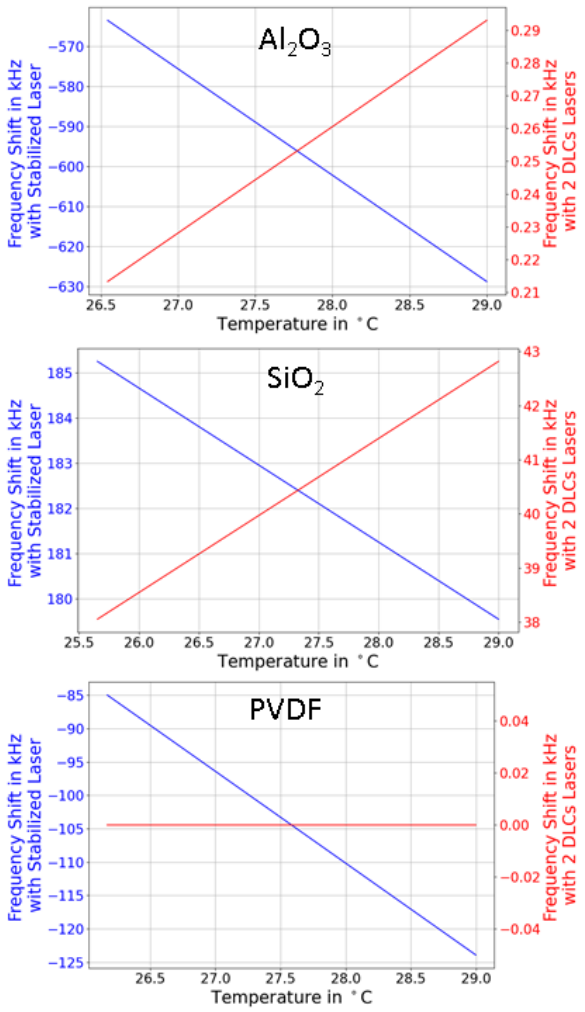

Figure 5: Simulated sensitivities (frequency shift) with respect to temperature changes.

The simulation for the PVDF shows no change in the beat frequency between the two diode lasers. This is due to the non-birefringence (as both directions have the same refractive index). The lasers were simulated to illuminate the same part of the material, thus the changes in their optical path lengths must be the same.

3.2. Second Approach

The measuring of pressure using refractivity was made with the setup of the Figure 3. Obtaining the results of Figure 6 where the normalized pressure (green), normalized temperature (magenta), normalized beat frequency between two diode lasers, one polarized vertically and other horizontally to the axis of the spacer of the studied materials (red), and the normalized beat frequency between the stabilised HeNe-laser and one polarized diode laser (blue) are shown in order to show which dependence is larger. To these simulations a temperature Gaussian instability of 1 mK was introduced, so it is possible to see directly which phenomenon is dominant.

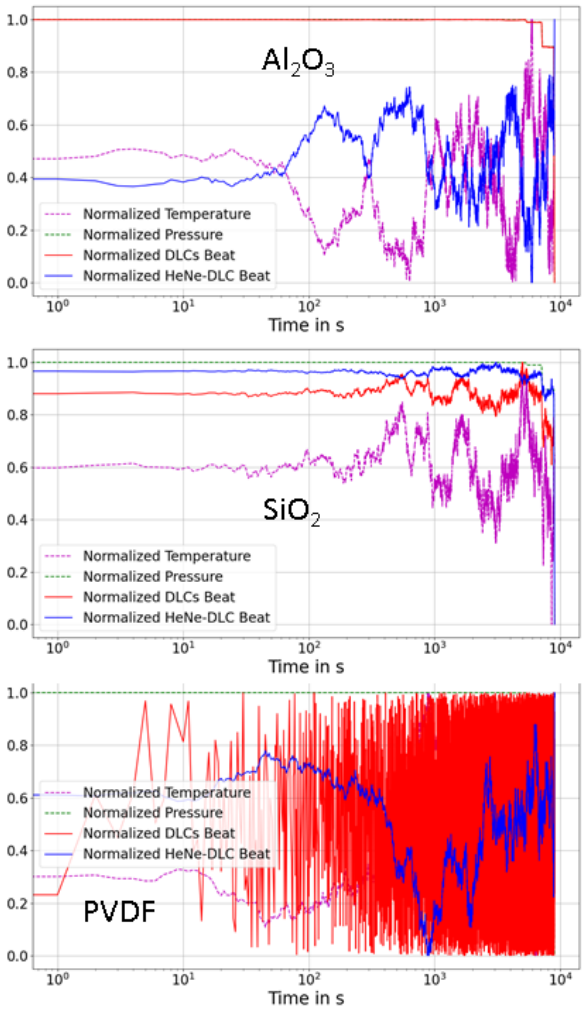

Figure 6: Simulated results of the change of beat frequency with a HeNe stabilised laser and two lasers, one polarized vertically and other horizontally to the axis of the spacer of the studied materials.

It was shown that for the case of the Sapphire (Al_2O_3) the beat between the two diode lasers is more sensitive to pressure and the beat between one diode laser and the stabilized HeNe-laser is more sensitive to temperature changes. However, it was shown that the change in beat frequency between the two diode lasers was smaller than the one including the stabilized HeNe-laser. For SiO_2 a mix between both phenomena is shown. For the PVDF, only noise is obtained for the beat between the two diode lasers due to the non-birefringence and it seems that the beat between the stabilised laser and the diode laser depends only on the temperature.

3.3. Third Approach

The simulation of the electrical response to the applied pressure was only carried out for PVDF and

SiO_2, as the Al_2O_3 bulk piezo-electric behaviour has no experimental support. As for the previous simulations a thermal Gaussian instability of 1 mK was introduced into the system. The proposed system is a parallel face capacitor with the piezo-electric material between the two faces. The results of these simulations are presented in Figure 7 where the quartz (SiO_2) shows almost no dependence with the temperature, due to its non-pyroelectric nature. Although a second order pyro-electric coefficient can be calculated through the piezo-electric coefficient, the thermal expansion coefficient and the compliance matrix, there are no consistent values in the bibliography.

With respect to PVDF a dependence in both factors is shown, but the pressure dependency is the dominant. It is important to remember that the pyro-electric effect depends on the change in temperature over time. So, a system with a better temperature stability will have remarkably less noise.

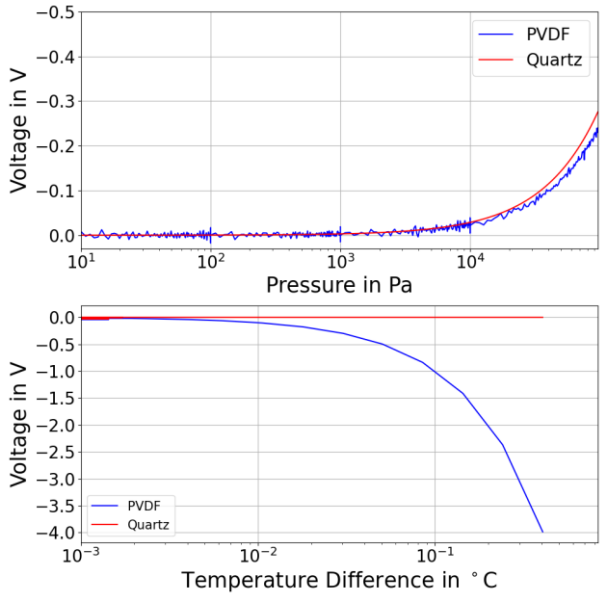

Figure 7: Electrical response to pressure with an additional thermal noise of 1 mK.

4. EXPERIMENTAL RESULTS FOR AL_2O_3

Sapphire was selected to carry out optical experiments, due to the different (by magnitudes) dependencies of the beat frequencies depending on the orientation of the crystal as shown in Figure 6.

Using a sapphire spacer inside a vacuum chamber (shown in Figure 8) optical measurements were made. Under the sapphire spacer an INVAR cavity was placed for subsequent measurements. In this chamber three parallel face condenser piezo-electric sensors made of PVDF (LTD0-028K) were placed, for testing the pressure measurement. Also, a PT100 sensor was placed inside for measuring the internal temperature, while the external temperature was measured with an external PT100 sensor which was in direct contact with the outer wall of the chamber. The inner gas pressure was measured with two Mensors heads (Type: CPT9000). The vacuum in the chamber was generated using a scroll pump and the pressure was introduced via loading the system using a Nitrogen 5.0 bottle (from Linde AG). The temperature of the gas was changed using a heat gun to heat the chamber. Later, some heating cables connected to a temperature controlled switch were added to heat the chamber in cycles with a timing of 2 min heating and 10 min cooling (turned off).

Figure 8: Vacuum chamber and Sapphire spacer.

In Figure 9 the evolution in time of the beat frequency between the stabilized HeNe-laser and a diode laser as well as the beat frequency between the two diode lasers is shown while heating and cooling the system. The diode lasers were locked to the maximum of intensity of the central interference caused by the superposition of the two reflections from the front end the backside of the sapphire spacer. Both diode lasers had different polarizations aligned with respect to the birefringence (c-axis) of the sapphire. The PT100 sensor positioned in space inside the vacuum chamber has a much smaller heat capacity, than the sapphire spacer. Therefore, the PT100 reacts immediately to the temperature changes due to the periodic heating of the chamber with the heating cables, while the sapphire takes more time to heat up and cool down. This can be easily seen from the corresponding peak to peak variations of the red and blue curves in Figure 9. It is clearly visible, that the changes in beat frequencies and in temperature are correlated. The sensitivity of the sapphire spacer was so high that mode jumps were required (to compensate for a limited tuning range), while only small changes in temperature were made. As it was shown in the simulations the change in beat frequency between both diode lasers (shown in green) is smaller than the change in the beat frequency between one diode laser and the stabilised HeNe-laser (shown in blue).

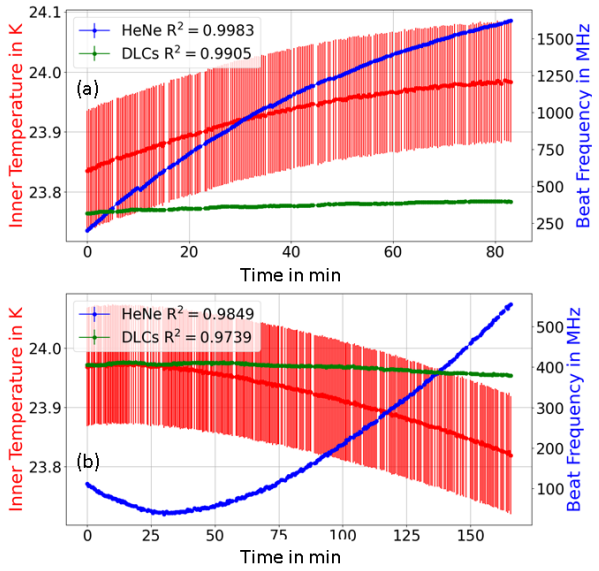

Figure 9: Evolution of the beat frequency between the stabilized HeNe-laser and a diode laser as well as the beat frequency between the two diode lasers when heating and cooling.

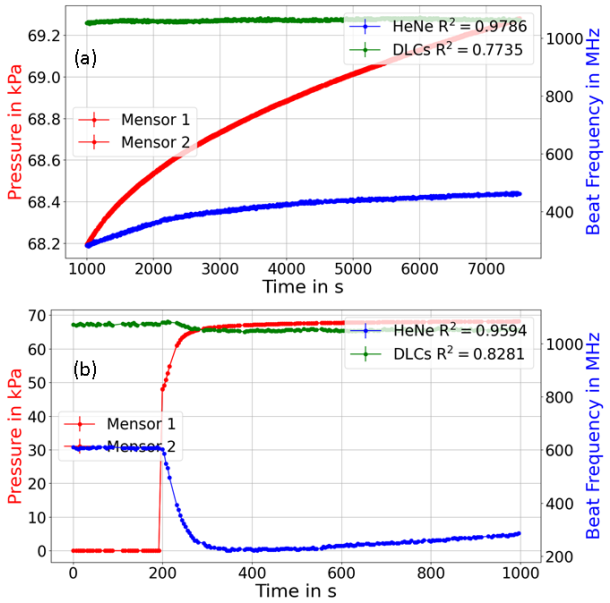

Figure 10: Evolution of the beat frequency between the stabilized HeNe-laser and one of the diode lasers as well as the beat frequency between the two diode lasers when changing the pressure.

In the Figure 10 the evolution of the beat frequency is shown when changing the pressure. The set-up for this experiment is the same as the one needed to obtain the data for Figure 9, so the diode lasers had different polarizations aligned with respect to the birefringence (c-axis) of the sapphire and they were locked to maximize the central intensity of the interference pattern. Unlike in Figure 9, here, the pressure uncertainties of the used mensor heads are low enough, so that a clear correlation can be found by the comparison to the values obtained via refractrometry. As it was shown before, the sensitivity of the beat between the diode lasers is lower than the sensitivity of the beat between the stabilized HeNe-laser and one of the diode lasers. In other words: Heating the sapphire causes a several times bigger relative change in its total optical path length compared to the relative change in the optical path lengths for both polarizations.

These are initial results which experimentally confirm the feasibility of the simultaneous temperature measurement (as planned by PTB) directly utilizing the FP-spacer which is part of the refractometer for the pressure measurements. A more in depth analysis will follow as well as further experiments at PTB.

With respect to the pressure-induced piezo-electronic measurements, a micro-voltmeter was used to measure the voltage generated by the LTD0-028K piezo-electric sensors. Although the resolution of the micro-voltmeter was not enough to solve small pressure variations, with greater pressure variations a signal was obtained indicating showing the feasibility.

5. SUMMARY

Simulations for 17 well-chosen materials were performed to estimate their sensitivities with respect to temperature and pressure changes, while the needed parameters were gathered within a literature review conducted for this purpose.

Sapphire is a material that can be used for measuring temperature and pressure. Quartz (SiO_2) has a mixed dependency on pressure and temperature changes, although it is more sensitive to temperature changes. Finally, PVDF can be used for accompanying piezo-electrical measurement of pressure.

Experimentally, the feasibility of using PVDF-based piezo-electric sensors for the measurement of pressure was shown. Better results can be achieved in the future, by using thicker sensors producing stronger signals as well as utilizing more sensitive voltmeters.

For the first time a new direct and non-invasive assessment of temperature changes of a sapphire-based FP-spacer was presented (as used for the new pressure standards based on FP-refractometry). This method demonstrated a very high temperature sensitivity with a low noise-to-signal ratio. While the exact same measurement method (utilizing the inner full-material part of the sapphire spacer for additional beam paths to probe their refractivity) can be used for pressure measurements it is by far more sensitive to temperature changes and will therefore potentially be used via a feedback to thermally stabilize the refractometer at PTB in the future.

6. REFERENCES

[1] K. Jousten, J. Hendricks, D. Barker, K. Douglas, S. Eckel, P. Egan, J. Fedchak, J. Flügge, Chr. Gaiser, D. Olson, J. Ricker, T. Rubin, W. Sabuga, J. Scherschligt, R. Schödel, U. Sterr, J. Stone, G. Strouse, "Perspectives for a new realization of the pascal by optical methods", Metrologia, vol. 54, 2017, no. 6, p. 146.
DOI: 10.1088/1681-7575/aa8a4d

[2] The 18SIB04 QuantumPascal EMPIR project website. Online [Accessed 20230102]: https://www.ptb.de/empir2019/quantumpascal/

[3] J. Zakrisson, I. Silander, C. Forssén, Z. Silvestri, D. Mari, S. Pasqualin, A. Kussicke, P. Asbahr, T. Rubin, O. Axner, "Simulation of pressure-induced cavity deformation – the 18SIB04 Quantumpascal EMPIR project", Acta IMEKO, vol. 9, 2020, no. 5, pp. 281–286.
DOI: 10.21014/acta_imeko.v9i5.985

[4] T. Rubin, I. Silander, J. Zakrisson, M. Hao, C. Forssén, P. Asbahr, M. Bernien, A. Kussicke, K. Liu, M. Zelan, O. Axner, "Thermodynamic effects in a gas modulated Invar-based dual Fabry–Pérot cavity refractometer", Metrologia, vol. 59, 2022, no. 3, 035003.
DOI: 10.1088/1681-7575/ac5ef9

[5] M. Born, E. Wolf, Principles of optics, 6th ed. United Kingdom: Pergamon Press Ltd., 1999. ISBN 0-08-026482-4

[6] J. Casas, Optica, 7th ed. Zaragoza: Librería Pons, 1994. ISBN 84-605-0062-4

[7] D. E. Gray, American Institute of Physics Handbook, 2nd ed. New York: McGraw-Hill Book Company, 1972. ISBN 07-001485-X

[8] C. Kittel, Introduction to Solid State Physics, 8th ed. Hoboken, NJ: John Wiley & Sons, Inc, 2005. ISBN 0-08-026482-4

[9] M. J. Weber, Handbook of Optical Materials. Boca Raton, Florida: CRC PRESS, 2003. ISBN 978-0-8493-3512-9